HHS Public Access

Author manuscript

J Bone Miner Res. Author manuscript; available in PMC 2015 August 25.

Published in final edited form as:

J Bone Miner Res. 2007 February ; 22(2): 274–285. doi:10.1359/jbmr.061110.

Marked Disturbance of Calcium Homeostasis in Mice With Targeted Disruption of the *Trpv6* Calcium Channel Gene

Suzy DC Bianco[1], **Ji-Bin Peng**[1], **Hitomi Takanaga**[1], **Yoshiro Suzuki**[1], **Alessandra Crescenzi**[1], **Claudine H Kos**[1], **Liyan Zhuang**[2], **Michael R Freeman**[2], **Cecilia HA Gouveia**[3], **Jiangping Wu**[4], **Hongyu Luo**[4], **Theodora Mauro**[5], **Edward M Brown**[6], and **Matthias A Hediger**[1]

[1]Membrane Biology Program and Renal Division, Brigham and Women's Hospital, Harvard Medical School, Boston, Massachusetts, USA

[2]Urological Diseases Research Center, Children's Hospital & Harvard Medical School, Boston, Massachusetts, USA

[3]Department of Anatomy, Institute of Biomedical Sciences, University of Sao Paulo, Sao Paulo, Brazil

[4]Laboratory of Immunology, Centre de Recherche, Centre Hospitalier de l'Universite de Montreal, Montreal, Canada

[5]Department of Dermatology, UCSF, San Francisco, California, USA

[6]Division of Endocrinology, Diabetes and Hypertension, Brigham and Women's Hospital, Harvard Medical School, Boston, Massachusetts, USA.

Abstract

We report the phenotype of mice with targeted disruption of the *Trpv6* (*Trpv6* KO) epithelial calcium channel. The mice exhibit disordered Ca^{2+} homeostasis, including defective intestinal Ca^{2+} absorption, increased urinary Ca^{2+} excretion, decreased BMD, deficient weight gain, and reduced fertility. Although our *Trpv6* KO affects the closely adjacent *EphB*6 gene, the phenotype reported here is not related to *EphB*6 dysfunction.

Introduction—The mechanisms underlying intestinal Ca^{2+} absorption are crucial for overall Ca^{2+} homeostasis, because diet is the only source of all new Ca^{2+} in the body. *Trpv6* encodes a Ca^{2+}-permeable cation channel responsible for vitamin D–dependent intestinal Ca^{2+} absorption. *Trpv6* is expressed in the intestine and also in the skin, placenta, kidney, and exocrine organs.

Materials and Methods—To determine the in vivo function of TRPV6, we generated mice with targeted disruption of the *Trpv6* (*Trpv6* KO) gene.

Results—*Trpv6* KO mice are viable but exhibit disordered Ca^{2+} homeostasis, including a 60% decrease in intestinal Ca^{2+} absorption, deficient weight gain, decreased BMD, and reduced fertility. When kept on a regular (1% Ca^{2+}) diet, *Trpv6* KO mice have deficient intestinal Ca^{2+}

Address reprint requests to: Matthias A Hediger, PhD, Institute of Biochemistry and Molecular Medicine, University of Bern, Bühlstrasse 28, CH-3012 Bern, Switzerland, matthias.hediger@mci.unibe.ch.

The authors state that they have no conflicts of interest.

absorption, despite elevated levels of serum PTH (3.8-fold) and 1,25-dihydroxyvitamin D (2.4-fold). They also have decreased urinary osmolality and increased Ca^{2+} excretion. Their serum Ca^{2+} is normal, but when challenged with a low (0.25%) Ca^{2+} diet, *Trpv6* KO mice fail to further increase serum PTH and vitamin D, ultimately developing hypocalcemia. *Trpv6* KO mice have normal urinary deoxypyridinoline excretion, although exhibiting a 9.3% reduction in femoral mineral density at 2 months of age, which is not restored by treatment for 1 month with a high (2%) Ca^{2+} "rescue" diet. In addition to their deranged Ca^{2+} homeostasis, the skin of *Trpv6* KO mice has fewer and thinner layers of stratum corneum, decreased total Ca^{2+} content, and loss of the normal Ca^{2+} gradient. Twenty percent of all *Trpv6* KO animals develop alopecia and dermatitis.

Conclusions—*Trpv6* KO mice exhibit an array of abnormalities in multiple tissues/organs. At least some of these are caused by tissue-specific mechanisms. In addition, the kidneys and bones of *Trpv6* KO mice do not respond to their elevated levels of PTH and 1,25-dihydroxyvitamin D. These data indicate that the TRPV6 channel plays an important role in Ca^{2+} homeostasis and in other tissues not directly involved in this process.

Keywords

intestinal calcium absorption; renal excretion; *TRPV6*; alopecia; vitamin D

INTRODUCTION

Calcium is the most abundant ion in the body. It is present in all tissues and organs and is necessary for numerous vital functions such as cardiac and skeletal muscle contraction, neurotransmission, tissue differentiation, and cell metabolism. All bodily Ca^{2+} is acquired through absorption from the diet. The vast majority is stored in the bones and a small percentage is recycled daily.(1)

The extracellular concentration of Ca^{2+} is maintained within a narrow range by the orchestrated interactions of hormones, Ca^{2+} channels, transporters, and sensors. When serum Ca^{2+} concentration decreases, the levels of PTH and 1,25-dihydroxyvitamin D increase and activate mechanisms that shunt Ca^{2+} into the blood. These mechanisms include intestinal absorption of Ca^{2+} from the diet, Ca^{2+} reabsorption by the kidneys, and resorption of Ca^{2+} from the bones. Because the diet is the sole source of new Ca^{2+}, the mechanisms involved in intestinal Ca^{2+} absorption are key players in overall Ca^{2+} homeostasis. Alterations in intestinal absorption (and/or renal reabsorption) of ions often result in pathophysiological conditions.

Vitamin D–sensitive intestinal Ca^{2+} absorption is an active process whereby Ca^{2+} is absorbed through the transcellular pathway. This pathway is believed to be the primary mechanism for Ca^{2+} influx into the body under conditions of normal or low Ca^{2+} intake (e.g., luminal $[Ca^{2+}]$ in the millimolar or submillimolar range).(2) It requires at least three steps: (1) entry through the apical brush border membrane; (2) transport across the cell to the basolateral side of the epithelium; and (3) active extrusion into the bloodstream. Two epithelial Ca^{2+} channels, TRPV5 and TRPV6, are now considered key molecules in the active (transcellular) entry of Ca^{2+} across the apical epithelia of the kidney and gut. TRPV5

and TRPV6 belong to the vanilloid subfamily of the Transient Receptor Potential (TRP) superfamily, and are predominately expressed in Ca^{2+}-transporting epithelia. They share 75% homology with one another, but are <40% homologous to other TRP family members. Both TRPV5 and TRPV6 are responsive to 1,25-dihydroxyvitamin D and have been shown to be selective for Ca^{2+} in electrophysiological studies.[3,4] *Trpv5* expression is rather restricted to the kidney, where its levels are high, whereas *Trpv6* is abundantly expressed in the duodenum and upper jejunum, as well as in the developing kidney, but only moderately expressed in the adult kidney.[5] In addition, Trpv6 is expressed in the skin, placenta, and exocrine organs.[6]

To study the roles of TRPV6 in vitamin D–regulated intestinal Ca^{2+} absorption, we developed a *Trpv6* knockout (*Trpv6* KO) mouse. This animal model is also useful for characterizing the contributions of the TRPV6 Ca^{2+} channel to other sites where active Ca^{2+} transport is important, thereby unraveling the relevance of TRPV6 to Ca^{2+} homeostasis and physiology.

MATERIALS AND METHODS

Animals

The *Trpv6* KO mice used in this study were from our colony housed at the Harvard Institutes of Medicine Animal Facility and, unless otherwise stated, had free access to water and food. They were fed a high Ca^{2+} (2% Ca^{2+} and 1.25% P), low Ca^{2+} (0.25% Ca^{2+} and 0.4% P), no added Ca^{2+} (contaminant Ca^{2+} ~0.005–0.01%; 0.4% P), or regular Ca^{2+} (1% Ca^{2+}, 0.4% P) diet. All special diets were from Harlan-Teklad (Madison, WI, USA). The *Trpv6* KO mice were backcrossed with the C57/B6 mice for three generations. They still carried a mixed background of B6/129. Thus, we always bred heterozygous pairs and used the wildtype littermates as controls for all experiments described herein. All animal protocols used were approved by the Institutional Animal Care and Use Committee (IACUC) of the Center of Animal Resources and Comparative Medicine (ARCM) of the Harvard Medical School.

The *EphB6* KO mice used in this study carried the C57/B6 background. They were backcrossed to C57/B6 for eight generations. Age-matched C57/B6 (2.5–6 months old) were used as controls.

Reagents

Unless otherwise specified, all reagents were from Sigma-Aldrich (St Louis, MO, USA).

Targeting vector and generation of Trpv6 null mice

The targeting vector (Fig. 1A) was constructed using a short and a long arm of the *Trpv6* sequence flanking the Neomycin resistance gene. The short arm is a 762-bp fragment flanked by the *Trpv6* primer sequences “CATSA2” (5′-CTTTCAGATGTTCCAACACCTG-3′) and “CATSA1” (5′-CATCCTTAGGGGTCACATAGG-3′). This segment includes part of the sixth intron, the seventh and eighth exons, and part of the ninth *Trpv6* exon. The sequence includes the last

of a series of ankyrin repeats, the first transmembrane domain, and most of the first extracellular loop. It was inserted into the 5′-end of the Neo cassette using a *Hind*III site. The long arm is a 9.5-kb DNA fragment from a mouse genomic library. It was inserted into the targeting vector using an *Afl*II site. The sequence of the long arm was found to start in the 14th intron of the *EphB*6 gene, which is oriented tail to tail with *Trpv*6 in the mouse genome and is separated by 120 bp. As a result, most of the coding sequence of *Trpv6* (from transmembrane domain 2 to the end of the protein) was replaced by the *Neo* cassette. In addition, the last four exons of the *EphB*6 gene were also deleted. Ten micrograms of the targeting vector was linearized with *Not*I and transfected by electroporation into 129 SvEv embryonic stem cells. After selection in G418, surviving colonies were expanded and screened for homologous recombination by PCR using CATSA12 and Neo1 as primers. CATSA12 is the 23-bp fragment, 5′-CAGGCTTGGAATGATTCCTGGAG-3′, outside of the short arm and 170 bp upstream of CATSA2. Neo1 (5′-TGCGAGGCCAGAGGCCACTTGTGTAGC-3′) is located in the 5′-promoter region of the neo-cassette. Positive clones, recognized by the amplification of a 1.1-bp fragment, were microinjected into C57BL/6J blastocysts to generate chimeric mice with germline transmission of the disrupted gene.

EphB6 is not known to be involved in Ca^{2+} homeostasis, and it is not expressed in mouse intestine.[7] Although no Ca^{2+}-related abnormalities were reported in the *EphB6* null mice,[8,9] we tested the *EphB6* KO mice for some of the calcium abnormalities found in the *Trpv6* KO mice described here.

Genotyping

The wildtype *Trpv6* allele was amplified by PCR using P1 as forward primer (5′-AACCTGAAAGAGCCAGGGACTTTGGAAAC-3′) and P2 as reverse primer (5′-CGAGAATGGTCTGTCCAAAGAA TCGAGTG-3′). P1 is located in the 8th intron and P2 is located in the 10th exon of *Trpv6*. The expected product is 314 bp. The allele that was knocked out was amplified using P1 and P3 as primers, where P3 is identical to the Neomycin resistance cassette. The amplified product was 220 bp. Because the 10th *Trpv6* exon is deleted in the *Trpv6* KO mice, and the Neo cassette is absent in the WT mice, all primers were included in the same reaction mixture for routine genotyping. DNA amplified from heterozygous carriers yielded both fragments (314 and 220 bp).

Quantitative detection of Trpv6 mRNA by real-time PCR

Total RNA was isolated using Trizol (Invitrogen), according to the manufacturer's instructions. After checking integrity by electrophoresis, RNA samples were reverse-transcribed using the Superscript II Reverse Transcriptase (Invitrogen) according to the manufacturer's protocol. The amount of *Trpv5*, *Trpv6*, or GAPDH cDNA in each sample was determined by quantitative PCR using the LightCycler system (Roche) in 20 μl containing 2 μl of LightCycler PCR mix DNA master SYBRGreen I (Roche), 0.25 μM of primers [*Trpv5*: 5′-ATTGACGGACCTGCCAATTACAGAG-3′ (forward) and 5′-GTGTTCAACCCGTAAGAACCAACGTC-3′ (reverse); *Trpv6*: 5′-ATCGATGGCCCTGCGAACT-3′ (forward) and 5′-CAGAGTAGAGGCCATCTTGTTGCTG-3′ (reverse); and GAPDH: 5′-

TCACCATCTTCCAGGAGCG-3′ (forward) and 5′-CTGCTTCACCACCTTCTTGA-3′ (reverse)], 3 mM $MgCl_2$, and 2 μl of cDNA. After the initial denaturation at 95°C for 20 s, the samples were amplified as follows: denaturation at 95°C for 0 s (with a temperature transition rate of 20°C/s from last extension cycle), annealing at 62°C (*Trpv5* and *Trpv6*) or 60°C (GAPDH) with a temperature transition rate of 8°C/s, extension at 72°C for 20 s (25 s for GAPDH) with a temperature transition rate of 4°C/s, followed by the fluorescence detection at 86°C (*Trpv5* and *Trpv6*) or 85°C (GAPDH) for 3 s.

Trpv6 expression by in situ hybridization and Western blotting

Sense and antisense probes were created from plasmid constructs of *Trpv6* cDNA inserted into pGEMTeasy (Promega) and synthesized using the DIG RNA labeling kit (Roche). The *Trpv6* cDNA probe was linearized with *Sal*I (for sense) or *Not*I (for antisense). The *Trpv5* cDNA probe was linearized with *Sal*I (for sense) or *Apa*I (for antisense). cRNA probes were transcribed from a fragment containing 670 kb (1934–2603) of the *Trpv6* cDNA and 943 kb (1963–2905) of the *Trpv5* cDNA, both flanked by promoter sequences of the T7 RNA polymerase for sense and SP6 RNA polymerase for antisense. Sense and antisense DIG-labeled transcripts were alkali-hydrolyzed to an average length of 500 nucleotides. In situ hybridization was performed on 10-μm cryosections of fresh-frozen mouse tissues. Sections were immersed in slide mailers in a hybridization solution composed of 50% formamide, 5% SSC, 2% blocking reagent (Roche), 0.02% SDS, and 0.1% *N*-lauroylsarcosine and were hybridized at 70°C for 60 minutes with sense or antisense probes at a concentration of 200 ng/ml. Sections were washed three times in 2% SSC and twice in 0.2% SSC for 30 minutes at 70°C. After washing, the hybridized probes were visualized by alkaline phosphatase histochemistry using alkaline phosphatase–conjugated, anti-digoxigenin Fab fragments (Roche) and 5-bromo-4-chloro-3-indolyl phosphate/nitro blue tetrazolium.

Protein expression was detected in enterocytes isolated from 6-month-old females by Western blot. Briefly, the first 15 cm of the small intestine was removed and rinsed. The epithelial layer was isolated and digested at 25°C × 200 rpm for 20 minutes in 0.1 M PBS with 1% NP-40, 0.25% sodium deoxycholate, 0.5% Triton X-100, and protease inhibitors (Roche). Digested layers were centrifuged at 15,000 rpm for 30 minutes at 4°C. Thirty micrograms of supernatant protein (Bradford) was submitted to 0.1% SDS/7.5% PAGE and transferred to a 0.45-μm nitrocellulose membrane (Pierce). Nonspecific binding was blocked with 0.5% Tween-20 and 2% skim milk in 0.1 M PBS, pH 7.4, for 30 minutes. Immunoreactive *Trpv6* was detected using a 1:5000 dilution of a polyclonal chicken anti-Trpv6 anti-serum in PBS[6] and 0.5% Tween-20 overnight at 4°C. The primary antibody was detected with a 1:5000 dilution of a horseradish peroxidase (HRP)-labeled goat anti-chicken antibody (Aves Laboratories) for 2 h at room temperature. The secondary antibody was washed and the labeled *Trpv6* was visualized by enhanced chemiluminescence (ECL detection system by Amersham Biosciences) according to the manufacturer's instructions.

Ca^{2+} gradient in the layers of stratum corneum

Skin samples were removed and processed for ion capture cytochemistry, as previously described.[10] Samples were minced and immediately immersed in an ice-cold fixative containing 2% glutaraldehyde, 2% formaldehyde, 90 mM potassium oxalate, and 1.4%

sucrose, pH 7.4. After overnight fixation at 4°C in the dark, samples were postfixed in 1% osmium tetroxide containing 2% potassium pyroantimonate and routinely processed and embedded in an epon–epoxy resin mixture. Ultra-thin sections were double-stained with uranyl acetate/lead citrate and examined with a Zeiss electron microscope operating at 60 kV.

Trpv6 immunostaining

Human Normal-Grid multitissue slides obtained from Biomeda (Foster City, CA, USA) were deparaffinized in xylene and rehydrated in gradient alcohol and water. The slides were blocked in 5% BSA at room temperature and incubated overnight with chicken anti-*Trpv6* IgY CH2747 (1:300) at 4°C. After three washings, slides were incubated with a 1:1000 dilution of the HRP-conjugated donkey anti-chicken IgG (Aves Laboratories) for 1 h at room temperature. Immunoreactivity was detected with the DAB (3,3′-diaminobenzidine tetrahydrochloride)-Chromagen system (ABC Elite from Vector Laboratories). Controls for nonspecific immunoreactivity were performed with preimmune chicken IgY.

Serum and urine Ca^{2+}

Total serum or urinary Ca^{2+} was determined by the Stanbio (Liquicolor, cat no. 0150) colorimetric assay. Briefly, the Ca^{2+} was dissociated from binding proteins in an acidic solution and combined with ortho-cresolphthalein complexone to form a stable purple color. The absorbance at 550 nm is linear and proportional to the amount of Ca^{2+} upto 15 mg/dl. The Ca^{2+} concentrations in serum and urine were calculated from a standard curve and are presented as milligrams per deciliter.

Intestinal Ca^{2+} absorption after oral gavage

All mice were starved overnight before the gavage experiments. Serum $^{45}Ca^{2+}$ was determined after oral administration of 0.15 ml/ g BW of 15 mM Tris-HCl, pH 7.4, containing 100 μM $CaCl_2$, 125 mM $NaCl_2$, 1.8 g/liter fructose, and 20 μCi/ ml $^{45}Ca^{2+}$ to hand-restrained mice using a feeding needle. Blood samples were collected at 5, 10, and 15 minutes (tail bleeding) and at 30 minutes by cardiac puncture in IsoFlo-anesthetized mice. Ten microliters of serum or urine collected at the same time-points was counted by liquid scintillation (Packard Instruments), and the results are presented as nanograms $^{45}Ca^{2+}$per milliliter serum or urine. Mouse carcasses were discarded according to the Harvard Radiation Protection Office Guidelines. In terms of the total calcium concentration used in the gavage studies (100 μM), our strategy was to minimize the undesired calcium entry at higher calcium levels (>100 μM) through the paracellular pathway, but also to keep it not too far below the apparent Trpv6 K_m for calcium (440 μM for rats, 250 μM for humans).

Metabolic studies, osmolality, and deoxypyridinoline determination in the urine

The mice were housed overnight in individual metabolic cages (Nalgene) with free access to water and food. The amount of water and food consumed and the volume of urine per animal were recorded daily for 2–3 consecutive days. Urine samples from different animals were used to determine total Ca^{2+}, osmolality, creatinine, and deoxypyridinoline (DPD). Osmolality in 10 μl of urine was determined using a vapor pressure osmometer (Wescor).

The osmometer was calibrated against standard solutions just before use. The results are the mean ± SE of 10–20 samples (mmol/kg). Urinary creatinine levels in the *Trpv6* KO mice were determined by the Stanbio colorimetric assay and used to normalize the urine DPD. Creatinine levels in *EphB6* KO mice were determined by the Synchron LX20 Clinical System (Beckman/Couter). The urine DPD was determined by the Metra DPD EIA kit (Quidel) according to the manufacturer's instructions. Samples were transferred to a DPD monoclonal antibody-coated strip. DPD in the sample competes for the antibody with conjugated DPD-alkaline phosphatase, and the reaction is detected with a pNPP substrate. DPD levels were normalized to creatinine. Results are expressed as nmol DPD/mmol creatinine and represent the mean ± SD of 10–20 samples.

Intact PTH assay

PTH was determined using the two-site ELISA for quantitative determination of intact PTH (Immutopics International, cat no. 60–2300). Two goat polyclonal antibodies were used. One is biotinylated and recognizes the C-terminal portion (39–84) of the peptide. The other is conjugated with HRP and recognizes the N-terminal region (1-34). Twenty-five microliters of serum was incubated for 3 h at room temperature with both antibodies in a streptavidin-coated microtiter plate. The wells were washed five times and incubated with the HRP substrate at room temperature for 30 minutes. PTH was calculated by plotting the absorbencies at 450 nm against the standard curve. Results are expressed as picograms per milliliter serum.

1,25-dihydroxyvitamin D assay

1,25-dihydroxyvitamin D was determined by radioimmunoassay (RIA; Nichols Institute Diagnostics, cat no. 40–6090). 1,25-dihydroxyvitamin D was separated from other vitamin D metabolites and potential cross-reactants before the assay by immunoextraction of 200 μl of nonhemolyzed serum using a monoclonal 1,25-dihydroxyvitamin D antibody (depilation agent). The purified 1,25-dihydroxyvitamin D in the eluate was diluted 1:2 and quantitated by RIA using a polyclonal antibody and ^{125}I-labeled 1,25 dihydroxyvitamin D as the tracer. 1,25-dihydroxyvitamin D in unknown samples was calculated against the standards, and the results are presented as picograms of 1,25-dihydroxyvitamin D per milliliter serum.

BMD

Adult males fed the regular, high, or no added Ca^{2+} diet for 1 month were weighed and killed by Isoflorane (IsoFlo) exposure at exactly 95 days of age. The right femur was dissected, and BMD was assessed by DXA using the pDEXA Sabre Bone Densitometer and the pDEXA Sabre Software version 3.9.4 (Norland Medical Systems, Fort Atkinson, WI, USA), both specially designed for small animals. The research mode scan option was used in the measurements, and the pixel spacing was set to 0.5 × 0.5 mm and scan speed to 4 mm/s. BMD values are the average of measurements from three mice.

Statistical analysis

Differences were considered significant when $p \leq 0.05$ by two-way ANOVA (three or more groups) followed by the Newman-Keuls post-test for comparison. When comparing two

groups, significance was tested with the Student's *t*-test. All regression curves were calculated and traced by the GraphPad Prism.

RESULTS

Confirmation of the knockout of the Trpv6 gene

We used the duodenum to document the absence of *Trpv6* expression, because it is the most important intestinal segment for *Trpv6*-dependent Ca^{2+} absorption and has the highest levels of *Trpv6* expression along the intestine. In situ hybridization of WT duodenum showed a strong signal in the epithelial cells, whereas no signal was detected in *Trpv6* KO male or female mice (Fig. 1B, first row). In addition, no *Trpv5* RNA could be detected in the same sections (Fig. 1B, second row). The Western blot of WT intestine detected 2 *Trpv6*-positive bands at 110 and 145 kDa, whereas no bands could be detected in the membranes isolated from *Trpv6* KO mice (Fig. 1C). The two bands are caused by complex glycosylation of *Trpv6*. When expressed in *Xenopus* oocytes or mammalian cells, *Trpv6* migrates as two major bands, which represents the core-glycosylated and complex glycosylated forms of Trpv6 channel proteins, respectively (unpublished observations). The native *Trpv6* from mouse small intestine exhibited higher molecular weight bands than those expressed in transfected cells. This is likely because of the fact that proteins in native tissues can undergo more complex glycosylation. A similar phenomenon has been reported for other transport proteins, such as the thiazide sensitive Na-Cl co-transporter (NCC) in mouse kidney.[11] The absence of *Trpv6* expression was corroborated by real-time PCR using the intestine (Fig. 2A) and kidneys (Fig. 2B) of *Trpv6* KO mice.

Figure 2B shows that *Trpv5* mRNA in the kidney was 34% increased in *Trpv6* KO mice fed a regular (1%) diet and 20% decreased in *Trpv6* KO mice fed a low (0.25%) Ca^{2+} diet compared with WT littermates kept on the same diets. The high (2%) Ca^{2+} treatment had no significant effect on the level of *Trpv5* or *Trpv6* mRNA in the kidney compared with regular Ca^{2+} diet, confirming our previous observations.[5] In contrast, compared with a regular diet, *Trpv6* mRNA levels in the intestine of WT mice were 87.5% reduced in response to a high Ca^{2+} diet and 124% increased in response to a low Ca^{2+} diet (Fig. 2A).

Characterization of the Trpv6 KO phenotype

Mice with targeted disruption of the *Trpv6* gene have a normal life span, although they show signs of abnormal development early in life. They weigh less than their WT littermates throughout life and have impaired fertility. In contrast, *EphB6* KO mice up to 24 months of age have no obvious signs of abnormal development or fertility.[8,9]

The difference in weight gain between KOs and controls slowly increased with time (Fig. 3A). The switch to the low Ca^{2+} diet at the 12th week of the experiment did not significantly affect the weight gain in control or *Trpv6* KO mice (Fig. 3A). During the first week of the experiment, the KO mice weighed 11.3% less than the age-matched controls, and by the 20th week, they weighed 20.1% less. No difference in weight gain was observed between *Trpv6* KO and heterozygous mice.

When kept on a regular diet, *Trpv6* KO males rarely impregnated females: Only once was a KO male able to impregnate a heterozygous female, resulting in the birth of only one pup. KO females took longer to get pregnant than control females, and when they eventually became pregnant, they had a relatively small number of pups (usually four to six pups). About 20% of the KO mothers showed abnormal maternal behavior with at least part of the litter. Transferring KO mothers with abnormal maternal behavior to a new cage did not trigger pup retrieval or nest-building activities.

Eighty percent of all KO and 35% of all heterozygous mice exhibited alopecia as soon as their hair started to grow (Fig. 3B). These percentages decreased with age, and by adulthood, 20% of all *Trpv6* KO and 5% of all heterozygous mice had persistent alopecia and an eczematous dermatitis (Figs. 3C and 3D). However, only heterozygous mice born to KO mothers developed alopecia (e.g., no cases of alopecia in heterozygotes born to WT mothers were observed). Although we cannot exclude the possibility that there was increased maternal grooming, it has been shown that the mammary gland expresses high amounts of *Trpv6*,[6] suggesting that Ca^{2+} deficiencies in the milk may have been involved.

Analysis of skin samples from WT mice revealed the expected Ca^{2+} gradient in which the levels of intracellular and extracellular Ca^{2+} progressively increase from the basal layer to the uppermost viable epidermal layer, the stratum granulosum (Fig. 3Ea). In contrast, epidermis isolated from *Trpv6* KO mice exhibited a visible reduction in total Ca^{2+} with losses of intracellular as well as extracellular Ca^{2+}, particularly in the uppermost stratum granulosum where the normal Ca^{2+} concentration is well above the serum levels. These alterations were present not only in epidermal regions exhibiting alopecia, but also in *Trpv6* KO epidermis with normal appearance (Fig. 3Eb). Accordingly, epidermis from normal skin tissue show noticeable levels of *Trpv6* expression (Fig. 3F). The amount of lipid secretion and the degree of lipid processing, also required for normal epidermal permeability barrier function, appeared normal in both WT and *Trpv6* KO animals. Even though the *EphB6* KO mice show no signs of alopecia or dermatitis, skin samples of the *EphB6* KO mice are being analyzed and show no signs of abnormal Ca^{2+} gradient (data not shown). Although we cannot rule out the contribution of *EphB6* at this point, the striking similarities in the skin (as well as the overall Ca^{2+} homeostasis) phenotype of the *Trpv6* and VDR KO mice suggest that these epidermal defects may be related to a tissue-specific Ca^{2+} signaling deficiency.

Intestinal Ca^{2+} absorption

Intestinal $^{45}Ca^{2+}$ absorption was deficient in *Trpv6* KO mice under all conditions tested. The concentration of total calcium used (0.1 mM) is below the TRPV6 K_m and was chosen to ensure that the TRPV6-mediated uptake would not be saturated. Therefore, the results would reflect the uptake through TRPV6 calcium channels. In addition, this strategy minimizes the undesired entry of calcium through the paracellular pathway.

After oral administration of $^{45}Ca^{2+}$, *Trpv6* KO mice on the regular diet accumulated ~60% less $^{45}Ca^{2+}$ in the serum from 5 to 30 minutes than did their controls (Fig. 4A). When kept on a low (0.25%) Ca^{2+} diet, $^{45}Ca^{2+}$ accumulation in the KO mice was reduced by ~40% at 5 minutes, and it decreased further to 50% at 15 and 30 minutes (Fig. 4B). In addition, when kept on the regular (1%) diet, maximal serum $^{45}Ca^{2+}$ in all mice had not been reached by 30

minutes (Fig. 4A), although all kept on the low Ca^{2+} diet reached a peak of serum $^{45}Ca^{2+}$ on or around 15 minutes (Fig. 4B). In addition, feeding the low (0.25%) Ca^{2+} diet caused an increase in total Ca^{2+} absorbed at all time-points, regardless of the mouse genotype. In WT mice, this increase was ~7.5-fold, whereas in the *Trpv6* KO mice it was 9.6-fold, suggesting that a TRPV6-independent pathway may be stimulated by Ca^{2+} restriction and that the persistent ~60% deficit in Ca^{2+} absorption may represent the contribution of TRPV6 to the total intestinal Ca^{2+} absorption capacity.

Serum parameters

The serum intact PTH of *Trpv6* KO mice fed the regular diet was significantly (3.8-fold) elevated compared with their WT counterparts maintained on the same diet (Fig. 5A). When switched to the low (0.25%) Ca^{2+} diet, WT mice increased their serum PTH levels 4.2-fold, reaching levels not significantly different from those of *Trpv6* KO mice on the regular diet. This suggests that *Trpv6* KO mice on a regular diet (i.e., not challenged with low environmental Ca^{2+}) have maximally elevated serum PTH. When challenged with a low Ca^{2+} diet, *Trpv6* KO mice showed only a slight, nonsignificant increase in their intact PTH (Fig. 5A).

The serum 1,25-dihydroxyvitamin D followed a similar pattern: When on regular diet, *Trpv6* KO mice exhibited a 2.4-fold elevated serum 1,25-dihydroxyvitamin D. Switching WT mice to low Ca^{2+} diet caused a 2.3-fold increase in their serum concentration, whereas *Trpv6* KO were unable to generate any further increase (Fig. 5B). *Trpv6* KO mice on regular diet are normocalcemic (Fig. 5C). However, when challenged with the low Ca^{2+}, they fail to respond in the manner exhibited by their control littermates, ending up with significantly lower levels of serum Ca^{2+} (Fig. 5D). The average total serum Ca^{2+} in all groups fed the regular diet was ~9 mg Ca^{2+}/dl (Fig. 5C). When fed the low Ca^{2+}diet, WT mice increased their serum Ca^{2+} to 10.3 mg/dl, whereas *Trpv6* KO mice did not (Fig. 5D). The elevated serum Ca^{2+} in WT mice on this diet was observed in every male and female based on five independent experiments. As internal controls, we ran serum samples of WT mice on a no added Ca^{2+} diet, because these mice did not exhibit any increase in serum Ca^{2+} levels.

Urinary parameters

Trpv6 KO mice show several signs of renal abnormalities. The urinary osmolality in WT mice remained nearly constant under all experimental conditions (1587, 1606, and 1688 mmol/kg for low [0.25%], regular [%], and high [2%] Ca^{2+} diet, respectively; Fig. 6A), whereas in *Trpv6* KO mice, the osmolality varied in direct proportion to the amount of Ca^{2+} in their diet (e.g., 677, 1005, and 1767 mmol/kg for mice maintained on the low, regular, and high Ca^{2+}, respectively; Fig. 6A). Only *Trpv6* KO mice fed the high Ca^{2+} diet had normal osmolality, suggesting that these mice are unable to properly concentrate their urine. In addition, *Trpv6* KO mice had a significantly elevated urinary Ca^{2+} (6.61 ± 0.38 versus 2.93 ± 0.29 μmol/day for the KO and WT, respectively; Fig. 6B). The changes in urinary volume in *Trpv6* KO mice were in the opposite direction of those observed in their WT controls under the same conditions (Fig. 6C), again suggesting abnormal urine concentration.

EphB6 has recently been shown to be expressed in adult mouse kidney and, whereas lacking the tyrosine kinase activity common to other members of its family,[12] was postulated to play a role in kidney function.[13] Therefore, we tested the *EphB6* KO mice for some of the altered urinary parameters found in the *Trpv6* KO mice to determine the contribution of each deleted gene. Our results show that the *EphB6* KO mice have normal urinary Ca^{2+} excretion (Fig. 6D), normal urine volume (Fig. 6E), and normal urine creatinine (Fig. 6F), indicating that the alterations in volume, osmolality, and Ca^{2+} excretion in the *Trpv6* KO mice are caused by the *Trpv6* deletion.

Bone parameters

The results of the DXA revealed that, at 95 days of age, *Trpv6* KO mice on regular diet exhibited a 9.3% decrease in femoral mineral density, which was not restored after treatment with the high (2%) Ca^{2+} diet for 1 month (Fig. 7A). In fact, this regimen increased the difference in femoral mineral density between the WT and *Trpv6* KO mice to 13%. This was unexpected because PTH and 1,25-dihydroxyvitamin D are suppressed on the high Ca^{2+} diet, and the expression of *Trpv6* is very low in this condition.[14] The WT group increased their bone mass by 11.5% after high Ca^{2+} treatment, whereas the increase in *Trpv6* KO mice was much lower. There was no significant difference in femoral mineral density among mice maintained on the no added Ca^{2+} diet for 1 month (Fig. 7A).

Urinary DPD, a marker of bone resorption, was not increased in *Trpv6* KO mice fed the regular diet, even though their serum PTH was elevated. To the contrary, DPD levels tended to decrease in the KO mice. Even when fed the low Ca^{2+} diet, *Trpv6* KO mice did not respond by increasing their bone resorption as would have been expected. These findings are in contrast to those observed with the WT mice, which promptly responded to the low Ca^{2+} by increasing DPD levels by ~80% (Fig. 7B), probably contributing to the elevated serum Ca^{2+} observed in these WT mice.

DISCUSSION

Mice with deletion of the *Trpv6* gene have a normal life span, although they exhibit multiple signs of Ca^{2+} deficiency and abnormal development. One of the hallmarks of the *Trpv6* KO mice is their slower rate of weight gain (Fig. 3A), even when the litter is being breastfed. The *Trpv6* KO mice show certain striking similarities to the vitamin D knockout mice (VDR KO), despite the significantly elevated serum 1,25-dihydroxyvitamin D and normal expression of the VDR in the *Trpv6* KO mice. These similarities include decreased intestinal Ca^{2+} absorption even with ample dietary Ca^{2+} availability, secondary hyperparathyroidism (increased serum PTH and 1,25-dihydroxyvitamin D), decreased BMD, alopecia, and other skin abnormalities revealed by electron microscopy. For instance, a significant percentage of the *Trpv6* KO mice develop persistent alopecia (Fig. 3B) and dermatitis (Fig. 3C), phenotypes associated with the vitamin D resistance caused by inactivating mutations of the VDR.[15–18] The detection of *Trpv6* expression in normal skin tissue (Fig. 3F) may explain the skin phenotype in both the VDR and the *Trpv6* KO mice. Accordingly, recent studies found multiple vitamin D–responsive elements in the promoter region of the *TRPV6* gene,[19,20] and alopecia is the only Ca^{2+}-related phenotype of the VDR KO mouse not

rescued by a high Ca^{2+} diet, suggesting a tissue-specific deficiency. These findings suggest that there is a link between TRPV6 and vitamin D–regulated Ca^{2+} transport, normal hair growth, and the modulation of keratinocyte proliferation and differentiation. The Ca^{2+} concentration in the upper stratum granulosum is >1.4 mM,[21] which is above the free serum Ca^{2+}, indicating the presence of an active mechanism of Ca^{2+} transport. Loss of skin Ca^{2+} is observed in the abrogation of the epidermal permeability barrier,[22] as well as in skin diseases, such as psoriasis and Hailey-Hailey disease.[23,24] The *Trpv6* KO mice, however, have a disrupted skin Ca^{2+} gradient in the absence of dermatitis or alopecia (Fig. 3Eb), indicating an intrinsic inability to properly concentrate Ca^{2+} and suggesting that TRPV6 is involved in transporting Ca^{2+} into the epidermal keratinocytes. Further studies are needed to establish the exact role of TRPV6 in epidermal function.

The TRPV6 channel plays an important role in the vitamin D–stimulated intestinal Ca^{2+} absorption and its intestinal expression is stimulated by VDR activation.[4] Consistent with this, *Trpv6* expression in two strains of VDR KO mice is <10% of the normal levels,[14] and the intestinal Ca^{2+} absorption in VDR KO mice is substantially decreased, suggesting that disruption of TRPV6 impairs vitamin D–dependent stimulation of intestinal Ca^{2+} absorption. Accordingly, the *Trpv6* KO mice exhibit a substantial decrease in intestinal Ca^{2+} absorption under all conditions tested (Figs. 4A and 4B), despite their elevated serum 1,25-dihydroxyvitamin D levels. However, *Trpv6* KO mice were still able to proportionally increase Ca^{2+} absorption when switched to the low (0.25%) Ca^{2+} diet (compare Fig. 4B with 4A), suggesting that TRPV6-independent mechanisms also play a role. However, these TRPV6-independent mechanisms are not sufficient to maintain normal Ca^{2+} homeostasis, as indicated by the substantial secondary hyperparathyroidism and the inability of the *Trpv6* KO mice to respond to further Ca^{2+} challenges.

The purpose of the 0.25% Ca^{2+} diet was to disrupt Ca^{2+} balance in the *Trpv6* KO mice while being relatively mild and easily compensated for by the WT mice, providing at least one half of the daily Ca^{2+} requirement for WT mice. Accordingly, the WT mice promptly responded to this diet by elevating their serum PTH and 1,25-dihydroxyvitamin D levels, as well as increasing bone resorption and intestinal Ca^{2+} absorption. Conversely, *Trpv6* KO mice fed this low Ca^{2+} diet were unable to further elevate their serum PTH and 1,25-dihydroxyvitamin D levels, showed insufficient intestinal Ca^{2+} absorption, and did not increase their bone resorption. Interestingly, the WT mice on this diet also exhibited increased serum Ca^{2+}. This increase was consistently observed in all WT mice fed this diet. It should be noted that studies looking at the effects of low Ca^{2+} are usually performed with no or extremely low Ca^{2+} concentrations added to the diet.[5,14,25] Accordingly, WT mice fed the no added Ca^{2+} diet showed no increase in serum Ca^{2+}. Thus, we used serum from these mice as internal controls.

The kidneys of the *Trpv6* KO mice do not respond to the elevated PTH and vitamin D levels by upregulating renal Ca^{2+} reabsorption (Fig. 2B), as would have been expected. As a result, *Trpv6* KO mice waste Ca^{2+} in the urine (Fig. 6B), suggesting abnormal renal handling of Ca^{2+}. We detected only moderate levels of *Trpv6* in the kidney,[5] (Fig. 2B), and another study found significant amounts of protein and RNA along the nephron.[26] However, all data published to date indicate that *Trpv5* is the gatekeeper of the active Ca^{2+} reabsorption

by the kidney.[2,27,28] Accordingly, Hoenderop et al.[29] showed that *Trpv5* KO mice waste Ca^{2+} in the urine, excreting as much as 6-fold more than their WT littermates. *Trpv5* KO mice, however, can compensate for this renal wasting with a 6-fold increase in the duodenal expression of *Trpv6* and a resultant marked increase in intestinal Ca^{2+} absorption. Although exhibiting a 3-fold increase in serum 1,25-dihydroxyvitamin D, *Trpv5* KO mice had no significant changes in PTH levels and no profound bone abnormalities.[29] On the other hand, the kidney of the *Trpv6* KO mice does not respond to the Ca^{2+} wasting, showing no apparent signs of compensation. It is possible that other *Trpv5*-independent mechanisms of Ca^{2+} handling may also be impaired. Alternatively, *Trpv6* expression in early kidney development could play a role. Although *Trpv6* expression in adult kidney is lower,[5,30] the situation during embryonic development is quite different: whereas *Trpv6* is expressed at high levels, *Trpv5* expression is much lower. It is around the time of weaning that this expression pattern is reversed: *Trpv6* expression falls, whereas *Trpv5* expression increases.[5] Alternatively, it is possible that the deficient Ca^{2+} reabsorption in *Trpv6* KO mice is exacerbated by direct effects of the marked hypercalciuria on the renal tubule (e.g., inhibition of water reabsorption mediated through the Ca^{2+}-sensing receptor) and that deposition of Ca^{2+} salts within the parenchyma may promote abnormal tubular function.

The *Trpv6* KO mice also carry a partial deletion of a second gene located adjacent to and aligned tail to tail with the *Trpv6* gene. This adjacent gene encodes *EphB6*, a kinase-defective *EphB* member of the tyrosine kinase *EphB* family.[12] This deletion was not intentional; however, we used the *EphB6* KO mice to measure some of the altered parameters found in our *Trpv6* KO mice for comparison. Mice with deletion of the *EphB6* gene do not have any obvious abnormalities related to Ca^{2+} homeostasis or development up to 24 months of age.[8,9] *EphB6* is highly expressed in the developing and adult brain and thymus, and at much lower levels in other tissues such as lung and kidney.[31] Members of the *EphB* family with tyrosine kinase activity have been shown to play a role in brain development and function, whereas the kinase-deficient *EphB6* has been shown to promote cell adhesion and migration in transfected HEK cells[31] and in the immune responses in mice.[9] *EphB6* KO mice have normal thymocytes subpopulations, thought to be caused by compensation by the overlapping expression of other members of the *EphB* family,[8,9] although the immune response of their mature T cells is compromised.[9] On the other hand, the *EphB6* KO mice have no signs of an abnormal skin phenotype.[7] They have normal Ca^{2+} excretion, urine volume, and creatinine concentration (Figs. 6D, 6E, and 6F, respectively), even though *EphB6* has been shown to be expressed in adult mouse kidney, and was suggested to contribute to the regulation of ion transport along the nephron.

The significant lower BMD observed in the *Trpv6* KO mice on regular diet (Fig. 7A) would be an expected consequence of an increased bone resorption caused by the elevated circulating PTH and 1,25-dihyrdoxyvitamin D levels found in these mice, thereby generating a negative Ca^{2+} balance in their bones. Conversely, urine levels of DPD were not altered in *Trpv6* KO mice, suggesting skeletal resistance to activation of bone resorption by PTH and vitamin D. This, in turn, suggests that the decreased BMD in the *Trpv6* KO mice may not be caused by enhanced bone resorption. Interestingly, Nijenhuis et al.[26] detected *Trpv6* expression in bone tissue, raising the possibility of a role of *Trpv6* in bone

homeostasis that could explain the lower BMD in this mouse model. In addition, the failure of the high (2%) Ca^{2+} "rescue" diet to normalize the BMD in these KO mice suggests that they might have a bone formation/mineralization defect. Even when taking into account that the KO mice started the rescue diet with a lower absolute BMD, the relative increase in their BMD after the high Ca^{2+} treatment was not comparable with that of their WT littermates. Furthermore, when challenged with a low Ca^{2+} diet, *Trpv6* KO mice did not increase their urinary DPD, thereby contributing to their subsequent hypocalcemia, whereas their WT littermates almost doubled their urinary DPD levels (Fig. 7B). These results indicate that the bones and kidneys of the *Trpv6* KO mice do not respond properly to PTH and 1,25-dihydroxyvitamin D, making these mice a unique model of bone and kidney resistance to PTH and vitamin D.

Some of the abnormalities observed in the *Trpv6* KO mice may be a result of Ca^{2+} deficiency during embryonic development through deficient maternal–fetal transfer of Ca^{2+}. The placenta exhibits exceptionally high levels of *Trpv6* expression in humans and mice.[3,32,33] It is well known that, in mammals, the Ca^{2+} concentration in the blood of the fetus is always higher than that in the maternal circulation.[34] To maintain this relative hypercalcemia, the transfer of Ca^{2+} from mother to fetus takes place against a Ca^{2+} gradient. In this context, *Trpv6* expression in the placenta is expected to enhance the rate of maternal transfer of Ca^{2+} to the fetus during pregnancy. In addition, *Trpv6* is known to be the target of the estrogen-induced increase in intestinal Ca^{2+} absorption during pregnancy to compensate for the higher maternal demand.[35] The pregnancy-specific deficiencies, combined with a decrease in intestinal Ca^{2+} absorption in the mother may lead to Ca^{2+} deficiency throughout embryonic development in *Trpv6* KO fetuses. A detailed study of fetal development in *Trpv6* KO mice is required and may uncover new roles of *Trpv6* in tissue differentiation and eventually help the understanding and prevention of diseases caused by Ca^{2+} deficiency and other abnormalities of Ca^{2+} homeostasis.

ACKNOWLEDGMENTS

This work was partially supported by NIH Grant CA101075. EMB was supported by NIH Grants DK52005 and DK67155. TM was supported by NIH Grant PO1AR39488.

REFERENCES

1. Frick KK, Bushinsky DA. Molecular mechanisms of primary hypercalciuria. J Am Soc Nephrol. 2003; 14:1082–1095. [PubMed: 12660344]
2. Peng JB, Brown EM, Hediger MA. Epithelial Ca2+ entry channels: Transcellular Ca2+ transport and beyond. J Physiol. 2003; 551:729–740. [PubMed: 12869611]
3. Peng JB, Brown EM, Hediger MA. Structural conservation of the genes encoding cat1, cat2, and related cation channels. Genomics. 2001; 76:99–109. [PubMed: 11549322]
4. Vennekens R, Hoenderop JG, Prenen J, Stuiver M, Willems PH, Droogmans G, Nilius B, Bindels RJ. Permeation and gating properties of the novel epithelial Ca(2+) channel. J Biol Chem. 2000; 275:3963–3969. [PubMed: 10660551]
5. Song Y, Peng X, Porta A, Takanaga H, Peng JB, Hediger MA, Fleet JC, Christakos S. Calcium transporter 1 and epithelial calcium channel messenger ribonucleic acid are differentially regulated by 1,25 dihydroxyvitamin D3 in the intestine and kidney of mice. Endocrinology. 2003; 144:3885–3894. [PubMed: 12933662]

6. Zhuang L, Peng JB, Tou L, Takanaga H, Adam RM, Hediger MA, Freeman MR. Calcium-selective ion channel, CaT1, is apically localized in gastrointestinal tract epithelia and is aberrantly expressed in human malignancies. Lab Invest. 2002; 82:1755–1764. [PubMed: 12480925]
7. Hafner C, Schmitz G, Meyer S, Bataille F, Hau P, Langmann T, Dietmaier W, Landthaler M, Vogt T. Differential gene expression of Eph receptors and ephrins in benign human tissues and cancers. Clin Chem. 2004; 50:490–499. [PubMed: 14726470]
8. Shimoyama M, Matsuoka H, Nagata A, Iwata N, Tamekane A, Okamura A, Gomyo H, Ito M, Jishage K, Kamada N, Suzuki H, Tetsuo NT, Matsui T. Developmental expression of EphB6 in the thymus: Lessons from EphB6 knockout mice. Biochem Biophys Res Commun. 2002; 298:87–94. [PubMed: 12379224]
9. Luo H, Yu G, Tremblay J, Wu J. EphB6-null mutation results in compromised T cell function. J Clin Invest. 2004; 114:1762–1773. [PubMed: 15599401]
10. Menon GK, Grayson S, Elias PM. Ionic calcium reservoirs in mammalian epidermis: Ultrastructural localization by ion-capture cytochemistry. J Invest Dermatol. 1985; 84:508–512. [PubMed: 3998499]
11. Kunchaparty S, Palcso M, Berkman J, Velazquez H, Desir GV, Bernstein P, Reilly RF, Ellison DH. Defective processing and expression of thiazide-sensitive Na-Cl cotransporter as a cause of Gitelman's syndrome. Am J Physiol. 1999; 277:F643–F649. [PubMed: 10516289]
12. Matsuoka H, Iwata N, Ito M, Shimoyama M, Nagata A, Chihara K, Takai S, Matsui T. Expression of a kinase-defective Eph-like receptor in the normal human brain. Biochem Biophys Res Commun. 1997; 235:487–492. [PubMed: 9207182]
13. Ogawa K, Wada H, Okada N, Harada I, Nakajima T, Pasquale EB, Tsuyama S. EphB2 and ephrin-B1 expressed in the adult kidney regulate the cytoarchitecture of medullary tubule cells through Rho family GTPases. J Cell Sci. 2006; 119:559–570. [PubMed: 16443753]
14. Van Cromphaut SJ, Dewerchin M, Hoenderop JG, Stockmans I, Van Herck E, Kato S, Bindels RJ, Collen D, Carmeliet P, Bouillon R, Carmeliet G. Duodenal calcium absorption in vitamin D receptor-knockout mice: Functional and molecular aspects. Proc Natl Acad Sci USA. 2001; 98:13324–13329. [PubMed: 11687634]
15. Hochberg Z. Vitamin-D-dependent rickets type 2. Horm Res. 2002; 58:297–302. [PubMed: 12446995]
16. Sultan A, Vitale P. Vitamin D-dependent rickets Type II with alopecia: Two case reports and review of the literature. Int J Dermatol. 2003; 42:682–685. [PubMed: 12956677]
17. Zlotogorski A, Hochberg Z, Mirmirani P, Metzker A, Ben Amitai D, Martinez-Mir A, Panteleyev AA, Christiano AM. Clinical and pathologic correlations in genetically distinct forms of atrichia. Arch Dermatol. 2003; 139:1591–1596. [PubMed: 14676077]
18. Bergman R, Schein-Goldshmid R, Hochberg Z, Ben Izhak O, Sprecher E. The alopecias associated with vitamin D-dependent rickets type IIA and with hairless gene mutations: A comparative clinical, histologic, and immunohistochemical study. Arch Dermatol. 2005; 141:343–351. [PubMed: 15781675]
19. Wang TT, Tavera-Mendoza LE, Laperriere D, Libby E, Macleod NB, Nagai Y, Bourdeau V, Konstorum A, Lallement B, Zhang R, Mader S, White JH. Large-scale in silico and microarray-based identification of direct 1,25-dihydroxyvitamin D3 target genes. Mol Endocrinol. 2005; 19:2685–2695. [PubMed: 16002434]
20. Meyer MB, Watanuki M, Kim S, Shevde NK, Pike JW. The human transient receptor potential vanilloid type 6 distal promoter contains multiple vitamin D receptor binding sites that mediate activation by 1,25-dihydroxyvitamin D3 in intestinal cells. Mol Endocrinol. 2006; 20:1447–1461. [PubMed: 16574738]
21. Lansdown AB. Calcium: A potential central regulator in wound healing in the skin. Wound Repair Regen. 2002; 10:271–285. [PubMed: 12406163]
22. Menon GK, Elias PM, Feingold KR. Integrity of the permeability barrier is crucial for maintenance of the epidermal calcium gradient. Br J Dermatol. 1994; 130:139–147. [PubMed: 8123567]
23. Menon GK, Elias PM. Ultrastructural localization of calcium in psoriatic and normal human epidermis. Arch Dermatol. 1991; 127:57–63. [PubMed: 1986708]

24. Hu Z, Bonifas JM, Beech J, Bench G, Shigihara T, Ogawa H, Ikeda S, Mauro T, Epstein EH Jr. Mutations in ATP2C1, encoding a calcium pump, cause Hailey-Hailey disease. Nat Genet. 2000; 24:61–65. [PubMed: 10615129]
25. Bouillon R, Van Cromphaut S, Carmeliet G. Intestinal calcium absorption: Molecular vitamin D mediated mechanisms. J Cell Biochem. 2003; 88:332–339. [PubMed: 12520535]
26. Nijenhuis T, Hoenderop JG, Van Der Kemp AW, Bindels RJ. Localization and regulation of the epithelial Ca2+ channel TRPV6 in the kidney. J Am Soc Nephrol. 2003; 14:2731–2740. [PubMed: 14569082]
27. Hoenderop JG, Nilius B, Bindels RJ. Calcium absorption across epithelia. Physiol Rev. 2005; 85:373–422. [PubMed: 15618484]
28. Nijenhuis T, Hoenderop JG, Bindels RJ. TRPV5 and TRPV6 in Ca(2+) (re)absorption: Regulating Ca(2+) entry at the gate. Pflugers Arch. 2005; 451:181–192. [PubMed: 16044309]
29. Hoenderop JG, van Leeuwen JP, van der Eerden BC, Kersten FF, Van Der Kemp AW, Merillat AM, Waarsing JH, Rossier BC, Vallon V, Hummler E, Bindels RJ. Renal Ca2+ wasting, hyperabsorption, and reduced bone thickness in mice lacking TRPV5. J Clin Invest. 2003; 112:1906–1914. [PubMed: 14679186]
30. van Abel M, Hoenderop JG, Bindels RJ. The epithelial calcium channels TRPV5 and TRPV6: Regulation and implications for disease. Naunyn Schmiedebergs Arch Pharmacol. 2005; 371:295–306. [PubMed: 15747113]
31. Matsuoka H, Obama H, Kelly ML, Matsui T, Nakamoto M. Biphasic functions of the kinase-defective Ephb6 receptor in cell adhesion and migration. J Biol Chem. 2005; 280:29355–29363. [PubMed: 15955811]
32. Peng JB, Chen XZ, Berger UV, Weremowicz S, Morton CC, Vassilev PM, Brown EM, Hediger MA. Human calcium transport protein CaT1. Biochem Biophys Res Commun. 2000; 278:326–332. [PubMed: 11097838]
33. Hirnet D, Olausson J, Fecher-Trost C, Bodding M, Nastainczyk W, Wissenbach U, Flockerzi V, Freichel M. The TRPV6 gene, cDNA and protein. Cell Calcium. 2003; 33:509–518. [PubMed: 12765696]
34. Kovacs CS, Kronenberg HM. Maternal-fetal calcium and bone metabolism during pregnancy, puerperium, and lactation. Endocr Rev. 1997; 18:832–872. [PubMed: 9408745]
35. Van Cromphaut SJ, Rummens K, Stockmans I, Van Herck E, Dijcks FA, Ederveen AG, Carmeliet P, Verhaeghe J, Bouillon R, Carmeliet G. Intestinal calcium transporter genes are upregulated by estrogens and the reproductive cycle through vitamin D receptor-independent mechanisms. J Bone Miner Res. 2003; 18:1725–1736. [PubMed: 14584880]

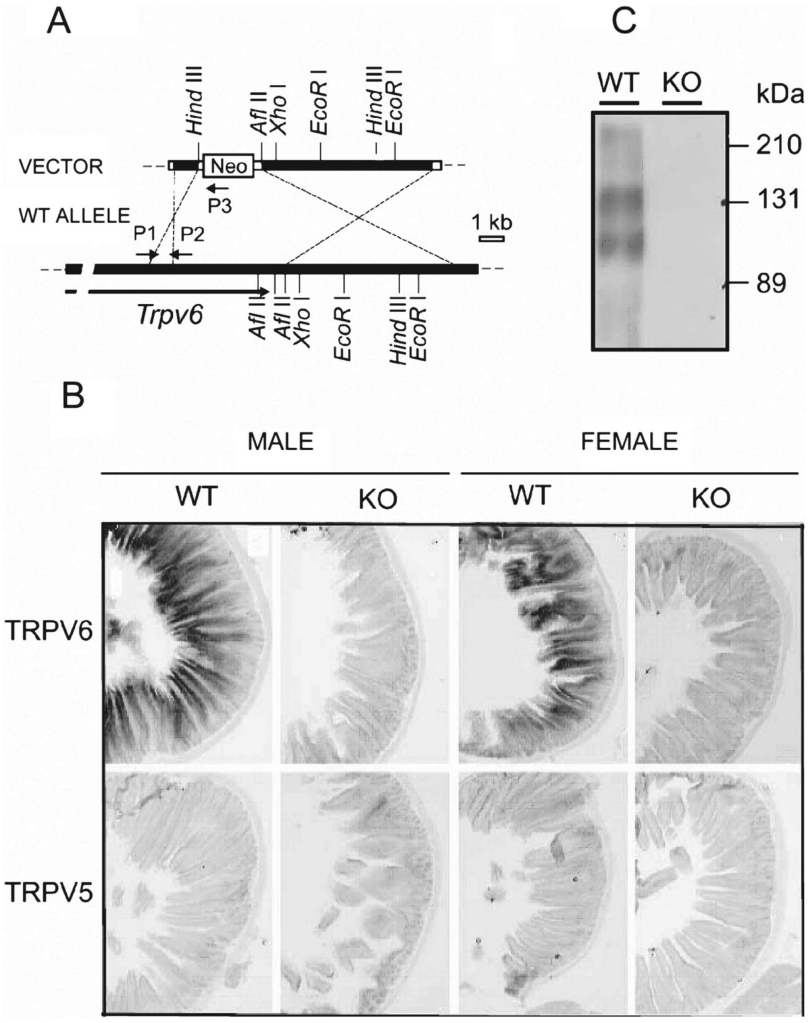

FIG. 1.

(A) *Trpv*6 targeting vector (top) and predicted product loci (bottom). P1, P2, and P3 indicate the positions of the primers used for genotyping. Filled boxes, exons with coding sequence; open boxes, exons for untranslated sequences (please refer to Materials and Methods section for details on the construction of the targeting vector). (B) In situ hybridization for *Trpv6* and *Trpv5* in the duodenum of adult wildtype (+) or *Trpv6* null mice (−) male (M) or female (F) mice ($^{-/-}$). (C) Western blot for *Trpv6* in the intestine of adult wildtype ($^{+/+}$) or *Trpv6* null mice.

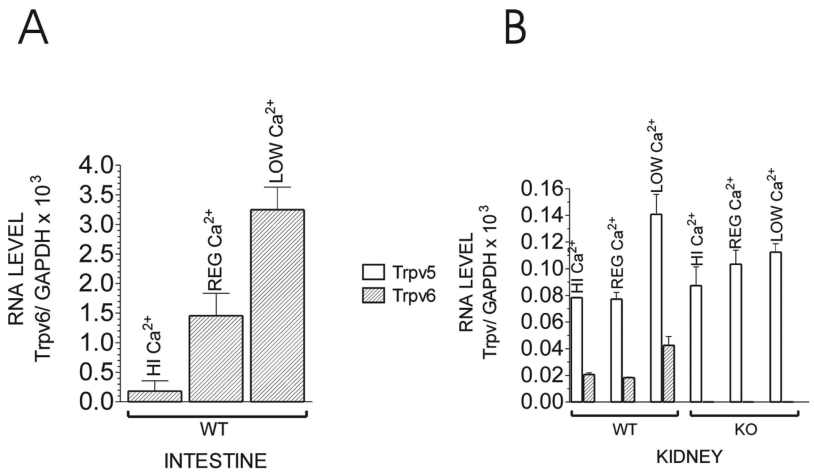

FIG. 2.

Quantitative RT-PCR for (A) *Trpv6* in the intestine and (B) *Trpv5* and *Trpv6* in the kidney of adult WT or *Trpv6* KO mice fed the low (0.25%), regular (1%), or high (2%) Ca^{2+} diet. Each bar is the average of two different mouse samples ± SE and is represented as the ratio of [Trpv/GAPDH] RNA × 10^3.

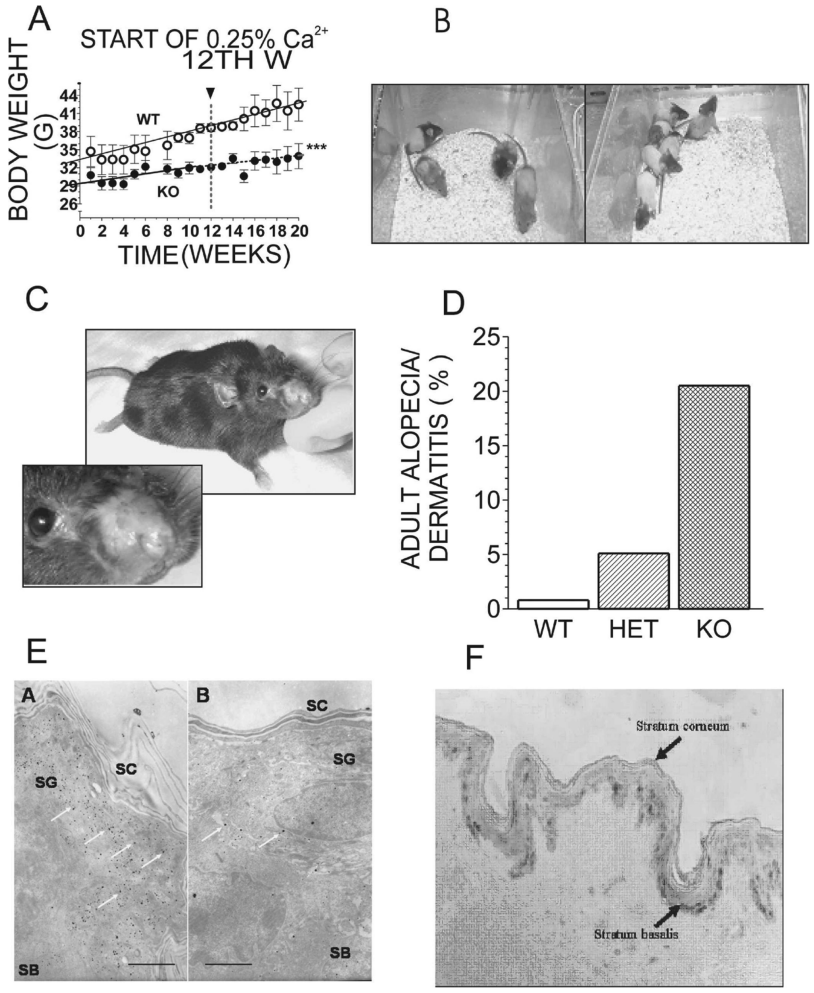

FIG. 3.

(A) Weight gain in adult WT or *Trpv6* KO mice fed the regular (1% Ca^{2+}) diet. At the 12th week of the experiment, the diet was switched to the low (0.25%) Ca^{2+} diet. Weight gain was recorded once a week, and the results are the average of 4 mice ± SE. ***$p < 0.0001$ vs. WT. (B) 25-day-old pups born to *Trpv6* $^{+/-}$ mothers bred on the high (2%) Ca^{2+} diet. (C) Adult (8 months old) *Trpv6* KO female with severe dermatitis of the nose. (D) Incidence of alopecia/dermatitis among adult *Trpv6* KO mice. Approximately 800 mice born to different combinations of breeding pairs were observed for 1 year. White bar, WT mice; striped bar, heterozygous (Het) mice; black bar, *Trpv6* KO (KO) mice. (E) Electron dense deposits of Ca^{2+} precipitates in normal-appearing skin of adult (a) WT and (b) *Trpv6* KO mice. White arrows, electron dense deposits; SG, density of Ca^{2+} precipitates in the stratum granulosum of the outer epidermis; SB, density of Ca^{2+} precipitates in the stratum basalis of the inner epidermis; SC, density of Ca^{2+} precipitates in the stratum corneum. Bars are 2 rm radium. (F) TRPV6 immunostaining in normal skin: Normal-Grid slides of skin tissue were incubated with anti-TRPV6, washed, and incubated with HRP-conjugated second IgG. Immunoreactivity was detected with the DAB-Chromagen system (ABC Elite). Controls for nonspecific immunoreactivity were performed with preimmune serum.

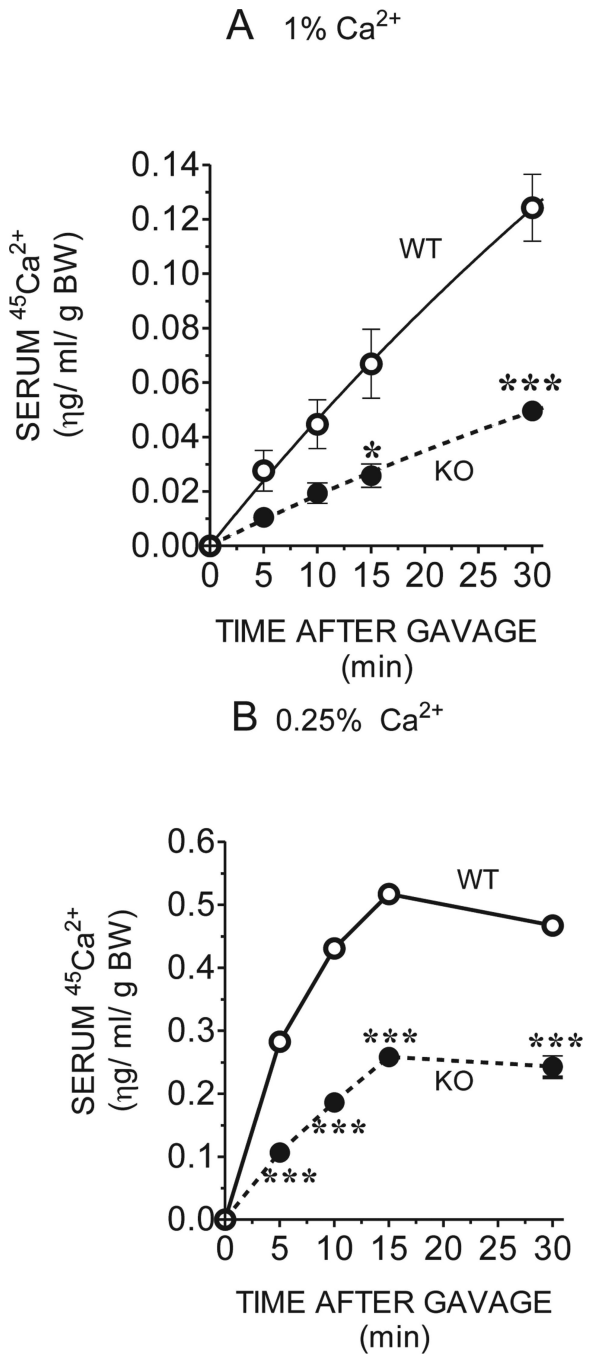

FIG. 4.

Concentration of $^{45}Ca^{2+}$ in the serum after oral gavage of adult WT or *Trpv6* KO mice fed the (A) regular (1%) or (B) low (0.25%) Ca^{2+} diet. Blood samples were collected at 0, 5, 10, 15, and 30 minutes after gavaging the mice with 15 μl/g BW of 15 mM Tris, 100 μM $CaCl_2$, 125 mM $NaCl_2$, 1.8 g/liter fructose, and 20 μCi/ml ^{45}Ca. Ten microliters of serum was counted, and $^{45}Ca^{2+}$ concentration was calculated by plotting the counts against a $^{45}Ca^{2+}$ standard curve. Each point of the 1% Ca^{2+} curves is the average of five WT and three *Trpv6*

KO mice; for the 0.25% Ca^{2+} curves, each point is the average of three WT and two *Trpv6* KO mice ± SE. *$p < 0.05$; ***$p < 0.0001$ vs. WT controls in the same diet.

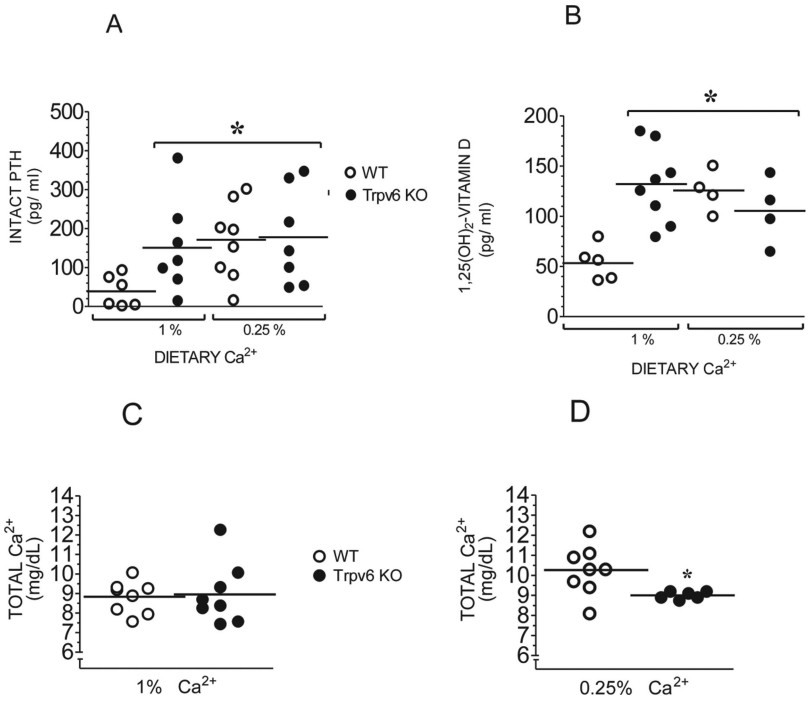

FIG. 5.

(A) Intact PTH and (B) 1,25 dihydroxyvitamin D in the serum of adult mice fed the regular (1%) or low (0.25%) Ca^{2+} diet. Total Ca^{2+} in the serum of adult WT or *Trpv6* KO mice fed a (C) regular (1%) or (D) low (0.25%) Ca^{2+} diet was assessed by colorimetric assay. Absorbencies were plotted against a standard Ca^{2+} concentration curve. Results from each group represent the mean ± SE of at least 10 serum samples from different mice. $*p < 0.05$ vs. WT in regular diet.

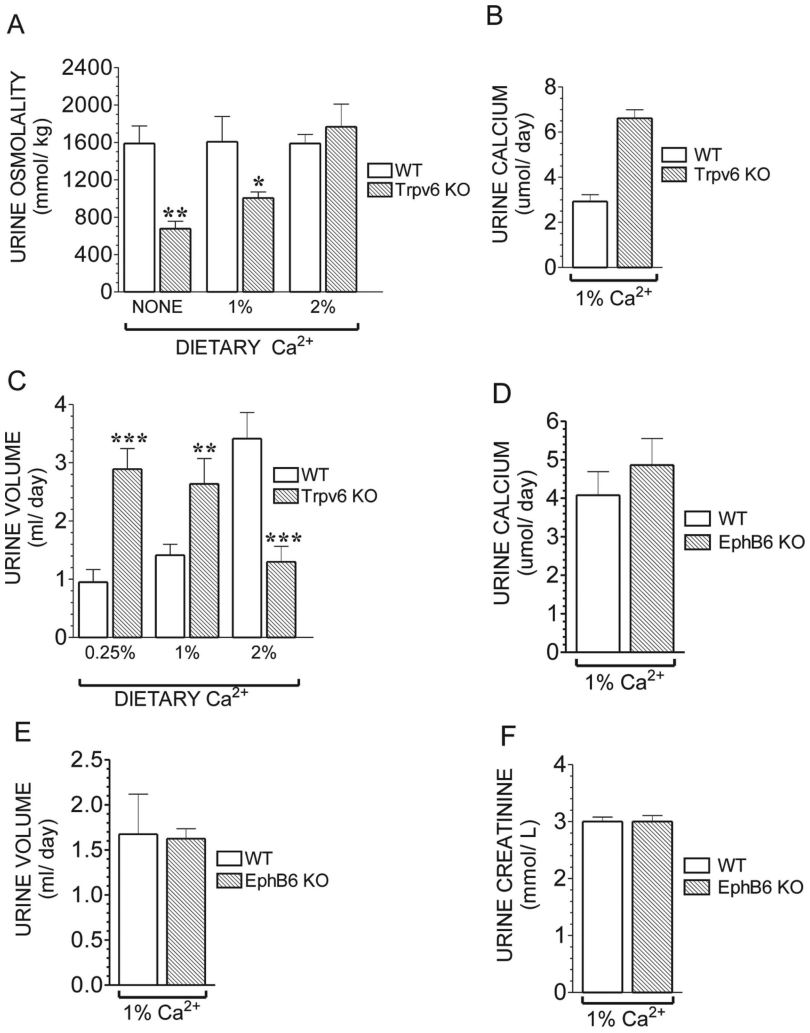

FIG. 6.

(A) Urine osmolality in adult WT or *Trpv6* KO mice fed a no added Ca^{2+}, regular (1%), or high (2%) Ca^{2+} diet. Osmolality was measured in a vapor pressure osmometer. Values are the mean ± SE of urine samples from six WT and six *Trpv6* KO mice. (B) Urine Ca^{2+} in adult *Trpv6* KO fed a regular Ca^{2+} diet. Ca^{2+} concentration was determined by a colorimetric assay. Values are the mean ± SE of urine samples from three WT and three *Trpv6* KO mice. (C) Daily urine volume in adult WT or *Trpv6* KO mice fed a low (0.25%), regular (1%), or high (2%) Ca^{2+} diet. Values are the mean ± SE of urine samples from seven WT and seven *Trpv6* KO mice. All samples were collected after 3 months of diet treatment. Open bars, WT mice; black bars, *Trpv6* KO mice. (D) Daily urine Ca^{2+} excretion in adult *EphB6* KO mice fed a regular diet. (E) Daily urine volume in adult *EphB6* KO mice fed a regular Ca^{2+} diet. (F) Urine creatinine levels in adult *EphB6* KO mice fed a regular Ca^{2+} diet. The urine results from *EphB6* mice represent the mean ± SE of urine samples from seven WT (14 samples collected in 2 different days) and four *EphB6* KO mice (8 samples collected in 2 different days). *$p < 0.05$ vs. WT in the same diet; *$p < 0.05$ or **$p < 0.001$ vs. WT in the same diet.

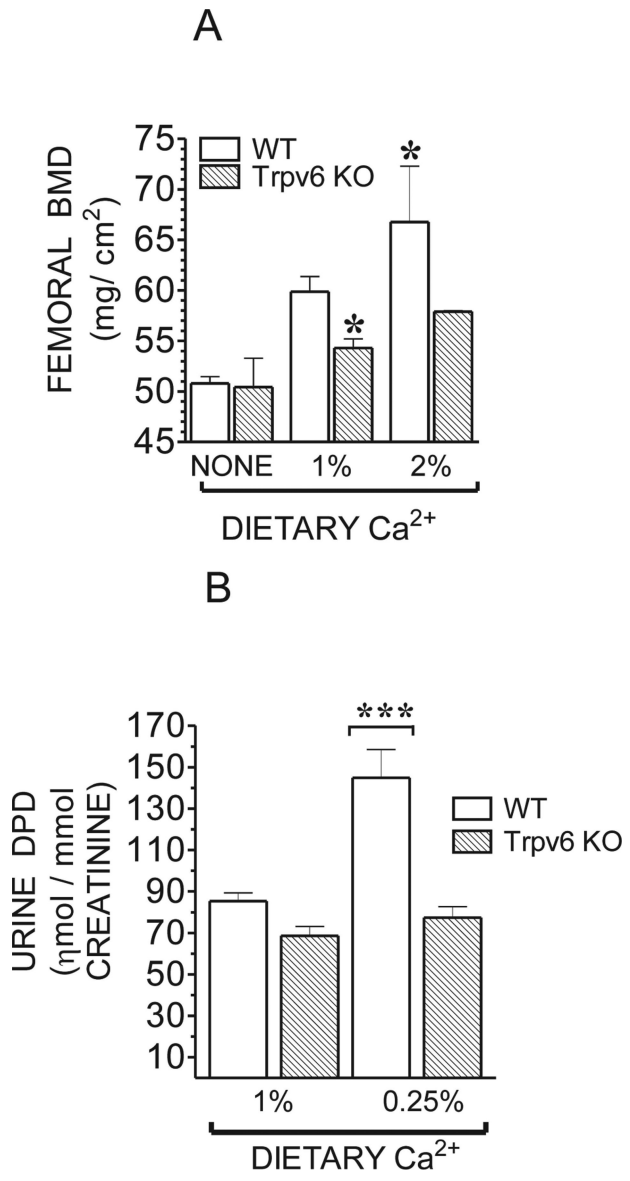

FIG. 7.

(A) BMD in adult *Trpv6* KO and WT littermates fed a no added Ca^{2+}, regular (1%), or high (2%) Ca^{2+} diet. BMD was assessed by DXA in the femora of 95-day-old male mice. Values are mean ± SE of three mice. (B) DPD concentration in urine samples from adult WT or *Trpv6* KO mice housed overnight in individual metabolic cages and fed a regular (1%) or low (0.25%) Ca^{2+} diet. Values are the mean ± SE of 10–15 samples collected from 10 mice. *$p < 0.05$ or ***$p < 0.0001$ vs. WT in regular diet.